Structure and dynamics of spherical crystals characterized for the Thomson problem

David J. Wales and Sidika Ulker

University Chemical Laboratories, Lensfield Road, Cambridge CB2 1EW, United Kingdom

Candidates for global minima of the Thomson problem for N charges on a sphere are located for $N \leq 400$ and selected sizes up to $N=972$. These results supersede many of the lowest minima located in previous work, with particularly large improvements for $N>400$. Our analysis reveals interesting topological defects, which are likely to play an important role in determining the mechanical and electrical properties of systems confined to a spherical geometry. We also find low-energy rearrangements for the Thomson model, an observation which suggests that suitable mesoscopic systems with analogous coarse-grained structure may exhibit fluxional dynamics.

The nature and concentration of defects governs characteristics such as mechanical strength, electrical conductivity, optical properties, and crystal growth rates. Flat two-dimensional surfaces can adopt a defect-free triangular lattice, where every particle has six nearest neighbors. However, for a spherical topology defects are an unavoidable consequence of geometry. If we write the particle coordination number as C, then the topological or disclination charge is defined as $Q=6-C$. Euler's theorem states that the total disclination charge must be 12 for the triangulated structure defined by a set of particles constrained to a spherical surface, but says nothing about how this condition is achieved. Hence characterizing the most favorable defects for systems with spherical topology is likely to play a key role in understanding and designing such materials.

The presence of 12 five-coordinate particles (fivefold *disclinations*) provides the simplest way for a spherical system to obey Euler's rule. However, as the number of particles increases, so does the strain energy associated with such arrangements. One way to reduce the strain energy is to introduce additional defects such as *dislocations*, which consist of adjacent vertices with fivefold and sevenfold coordination.[1–3]

Many examples of particles constrained to a roughly spherical or curved surface are known.[4–10] However, detailed atomistic modeling for most of these applications is not feasible. Instead, we can derive insight into possible generic features of systems with spherical topology, such as the most likely defect configurations, by considering N unit charges constrained to a sphere. The potential energy is therefore $\sum_{i<j} 1/|\mathbf{r}_i - \mathbf{r}_j|$, with $|\mathbf{r}_i|=1$ for all particles i and j. This model was first introduced by J. J. Thomson in 1904 in an effort to describe atomic structure.[11] Even for this simpler "Thomson problem" it is still quite challenging to determine the most favorable structure when N is of order 1000. In fact, the Thomson problem has served as a benchmark for global optimization algorithms in a number of previous studies.[12–19]

General arguments suggest that the number of local minima should increase exponentially with N.[15,20,21] However, this increase is slowest for long-range potentials,[15,20,21] because the corresponding minima are wider, and hence less numerous in configuration space. The present results indicate that basin-hopping global optimization[22–25] can provide very good candidates for global minima in the range $N<1000$. For $N \leq 200$ we identify a minimum at $N=188$, which im-

proves the previous energy by 0.027 atomic units.[17,26] For $201 \leq N \leq 400$ we find lower minima for 150 of the 200 sizes compared to previous results,[18,19,26] with energy differences up to around 0.3 atomic units. For larger sizes our structures are up to 2.5 atomic units lower in energy than previous suggestions[16,18,19,26] (Table I). Clearly, predicting details of the favorable geometry for larger systems requires systematic global optimization.

The present study employed the basin-hopping approach[22–25,27] using the GMIN program,[28] where Monte Carlo type steps are used to sample local minima on the potential energy surface. This approach is particularly attractive because it has very few adjustable parameters, and is therefore readily transferable between different systems.[24,25] We employed five basin-hopping runs for each size starting from different random configurations of positive charges on a unit sphere. Our initial survey used a fixed temperature of $T=0.05$ and 1000 basin-hopping steps in each run (atomic units are employed throughout). All five runs agreed up to $N=299$, except for $N=272$, which may have a multifunnel potential energy surface,[25] and could therefore provide a good benchmark for future work. These results confirm that the Thomson problem is significantly easier than global optimization for atomic clusters with a comparable number of degrees of freedom, as anticipated above.

We then refined the temperature parameter and the number of steps to try and ensure reliable results for larger sizes, and settled upon $T=0.045$ and 100 000 steps. Above $N=400$ we considered selected sizes where previous results are available for comparison.[18,19] For $N>400$ even 100 000 steps was not always sufficient to obtain agreement between all five runs, and we expect that some of these results may be improved in future work. However, we are confident that all the lowest-lying minima we have obtained are close enough to the global minima for our structural predictions to be relevant. All the results will be tabulated in the Cambridge Cluster Database.[29] Many of the structures have nontrivial point-group symmetries, in agreement with the conjecture that higher symmetry structures will either have particularly high or particularly low energies.[25]

Most global minima in the size range considered exhibit at least 12 five-coordinate ions (fivefold disclinations), while many also exhibit four- or seven-coordinate ions. The structures are best presented using a Voronoi construction, based

TABLE I. Improved global minima for the Thomson problem at selected sizes. The number of polygons refers to faces with 5, 6, and 7 sides in the corresponding Voronoi construction.

N	Energy (atomic units)	$\frac{(2E-N^2)}{N^{3/2}}$	Point group	Polygons		
				5	6	7
188	16249.2226789	−1.103901	D_2	12	176	0
206	19585.9558565	−1.103980	C_2	12	194	0
218	21985.2639489	−1.103998	C_2	12	206	0
229	24307.5993133	−1.104000	C_1	13	215	1
234	25401.9317866	−1.104099	C_2	12	222	0
241	26975.1902840	−1.104052	C_3	12	229	0
246	28128.0514643	−1.104070	D_2	12	234	0
252	29543.5228681	−1.104135	C_2	12	240	0
258	30994.2135775	−1.104119	C_2	12	246	0
264	32479.9081412	−1.104136	D_2	12	252	0
269	33744.8007328	−1.104143	C_1	12	257	0
312	45629.3138040	−1.104219	C_2	12	300	0
327	50199.5714196	−1.104287	C_2	12	315	0
362	61719.0519098	−1.104301	C_1	17	340	5
432	88353.7096820	−1.104425	D_3	24	396	12
482	110317.9966044	−1.104511	C_2	22	450	10
492	115005.0932623	−1.104528	C_2	24	456	12
522	129655.3224067	−1.104563	C_2	24	486	12
572	156036.2192910	−1.104626	D_3	24	536	12
612	178909.7952490	−1.104647	C_1	24	576	12
632	190936.2620761	−1.104684	T	24	596	12
642	197097.1993002	−1.104679	C_1	24	606	12
672	216169.9939945	−1.104693	C_1	24	636	12
732	256972.4358872	−1.104748	T	24	696	12
752	271360.9889196	−1.104754	C_2	24	716	12
762	278703.0608815	−1.104750	C_2	24	726	12
792	301319.8733917	−1.104779	T	24	756	12
812	316890.4580541	−1.104789	C_2	24	776	12
842	340985.6576387	−1.104785	C_1	24	806	12
912	400657.6165027	−1.104821	C_1	33	858	21
932	418594.2339500	−1.104834	C_1	35	874	23
972	455651.0809351	−1.104867	T_h	36	912	24

on polygons that partition the surface into regions where each point is closest to a given ion. Our results are broadly in agreement with trends predicted in previous work.[10,30–33] However, we have characterized several new defect motifs, and can now provide accurate energetics for the favored structures.

Minima with point groups O, D_{4d}, D_{2d}, and C_{2v} usually contain defects other than fivefold disclinations. For example, the pentagonal icositetrahedron found for $N=24$ has a Voronoi representation consisting of "tetrapentagon patches" arranged to give O symmetry (Fig. 1). Here the Voronoi pentagons are colored red and the hexagons green. These Voronoi constructions include four-connected vertices, and
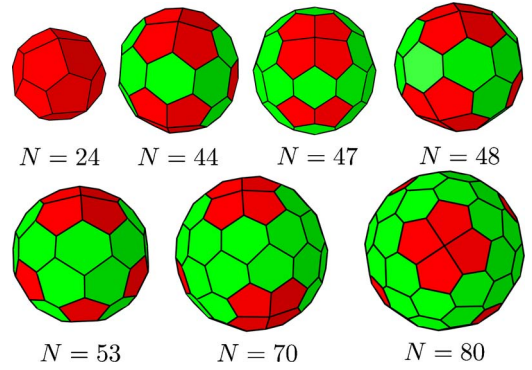

FIG. 1. (Color online) Voronoi representations of global minima for selected sizes that exhibit pentagon patches. $N=47$ also has a pentagon pair defect.

correspond to a face dual polyhedron with one or more square faces. Hence the topological charge calculated by summing the number of pentagonal faces is not equal to 12.

For larger systems we identify a defect based upon a 3×3 square of ions; examples occur for $N=141$, 166, 169, 170, 172, and 179 (Fig. 2). For this 3×3 defect the Voronoi assignment around the central ion is very sensitive to small changes in the geometry, and a real-space view may be more appropriate (Fig. 2). The heptagons shaded in blue for $N=126$ have two very short edges, which is why they look more like pentagons in the figure. This Voronoi construction has only three-connected vertices, and therefore corresponds to a topological charge of 12. There are two 3×3 defects, each with a overall charge of two, plus eight additional isolated pentagonal faces. For $N=141$ and $N=172$ the Voronoi representations include four-connected vertices, and $Q>12$.

The next defect we identify can be described as an extended dislocation, or scar,[31] and consists of a heptagon and two adjacent pentagons in the Voronoi representation. This defect carries a net topological charge of 1, and has been
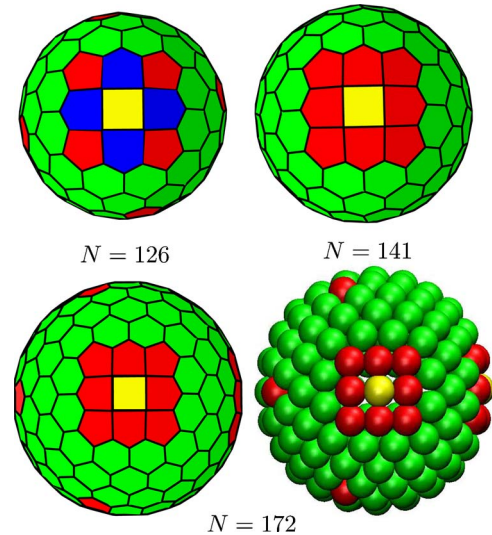

FIG. 2. (Color online) Global minima for selected sizes that exhibit the 3×3 defect. Both the Voronoi construction and a real-space view are shown for $N=172$.
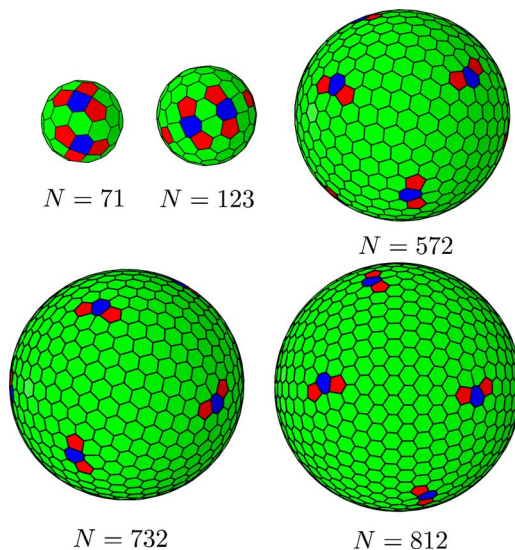
FIG. 3. (Color online) Global minima for selected sizes that exhibit extended dislocations consisting of a heptagon and two pentagons.

observed before in local minima.[19,31] In the global minima reported here, such features are prevalent for intermediate sizes, in agreement with recent predictions from a continuum elastic model.[31] The structures with 24 pentagons and 12 heptagons in Table I all feature this defect. Selected examples are illustrated in Fig. 3, including $N=71$, where additional pentagons are present and the two extended defects may be viewed in terms of distorted 3×3 patches. Our results indicate that extended dislocations are generally preferred over heptagon+pentagon pairs for most of the size range considered.

Extended dislocations could also be viewed as embryonic grain boundaries, which consist of pentagon-heptagon-pentagon-⋯ repeats.[32,33] The smallest size considered in the present study that exhibits a longer grain boundary is $N=792$, where pentagon pair defects and extended dislocations are also present (Fig. 4). All the larger global minima contain such features, but we also note the appearance of an alternative "twinned" defect (with a local mirror plane) in $N=912$, 932, and 972. Here two heptagons share an edge in the Voronoi construction, with three pentagons on the periphery. Each of these defects carries a net topological charge of 1. In previous experiments, grain-boundary scars were observed for self-assembled beads containing more than around
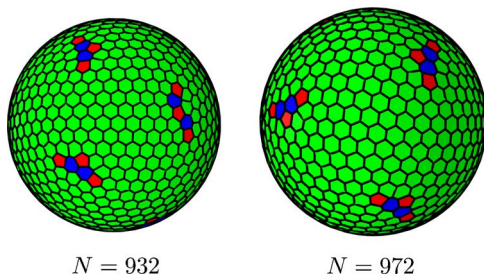

FIG. 4. (Color online) Global minima for selected sizes that exhibit grain boundaries and twinned grain boundaries.
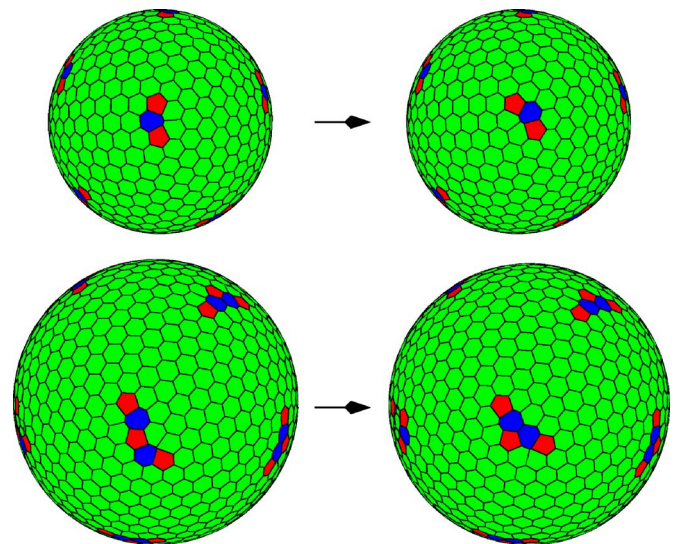

FIG. 5. (Color online) Defect migrations linking the global minimum to a low-lying local minimum for $N=732$ (top) and two low-lying minima for $N=972$ (bottom). The forward and reverse barriers in atomic units are 6.60×10^{-4} and 4.22×10^{-4} for $N=732$ and 4.24×10^{-3} and 1.04×10^{-3} for $N=972$.

360 particles.[4] For the Thomson problem our results suggest that extended dislocations of the pentagon-heptagon-pentagon variety are still favorable in this size range, and that grain boundaries and twinned grain boundaries become the preferred defects for $N>400$. Systematic global optimization therefore complements continuum models by providing accurate data for the defect energetics, and by revealing structures such as the 3×3 patches and twinned grain boundaries.

To characterize rearrangements between different local minima we have calculated transition states using hybrid eigenvector-following techniques,[34,35] as implemented in the OPTIM program.[28] Two examples are illustrated in Fig. 5 for migration of an extended dislocation in $N=732$ and interconversion of twinned and conventional grain boundaries in $N=972$. Our results indicate that low-lying minima for the Thomson problem can generally interconvert via relatively facile defect rearrangements. We therefore conclude that mesoscopic systems exhibiting coarse-grained structure corresponding to the Thomson problem could exhibit significant fluxionality. Hence suitable annealing could produce materials with uniform properties, a key goal of nanotechnology. The mesoscopic systems that might be relevant here would involve building blocks interacting via relatively isotropic forces, which might include multielectron bubbles in superfluid helium,[5,36] cell surface layers in prokaryotic organisms,[6,37] "colloidosomes,"[4,7,38] colloidal silica microspheres,[8] superconducting films,[10,39] and lipid rafts deposited on vesicles.[9] Rearrangements between fullerene cages, which have a dual topology to the Thomson problem and involve strong anisotropic covalent bonds, are known to have relatively high barriers.[40–42] Nevertheless, the organization of the energy landscape[42–44] is such that even here suitable annealing can produce a specific structure, i.e.,

icosahedral C_{60} (buckminsterfullerene).[45,46]

It is remarkable that the venerable Thomson problem is probably more relevant today than at any time since its inception as a model of atomic structure. Our study reveals defect structures and dynamics that are likely to be important in a variety of materials. In particular, the favored defects and their rearrangements will play a key role in determining observable mechanical, electrical, and optical properties.

[1] D. R. Nelson, *Defects and Geometry in Condensed Matter Physics* (Cambridge University Press, Cambridge, England, 2002).

[2] A. Pérez-Garrido and M. A. Moore, Phys. Rev. B **60**, 15628 (1999).

[3] A. Pérez-Garrido, Phys. Rev. B **62**, 6979 (2000).

[4] A. R. Bausch, A. C. M. J. Bowick, A. D. Dinsmore, M. F. Hsu, D. R. Nelson, M. G. Nikolaides, A. Travesset, and D. A. Weitz, Science **299**, 1716 (2003).

[5] P. Leiderer, Z. Phys. B: Condens. Matter **98**, 303 (1995).

[6] U. B. Sleytr, M. Sára, D. Pum, and B. Schuster, Prog. Surf. Sci. **68**, 231 (2001).

[7] T. Einert, P. Lipowsky, J. Schilling, M. J. Bowick, and A. R. Bausch, Langmuir **21**, 12076 (2005).

[8] Y.-S. Cho, G.-R. Yi, J.-M. Lim, S.-H. Kim, V. N. Manoharan, D. J. Pine, and S.-M. Yang, J. Am. Chem. Soc. **127**, 15968 (2005).

[9] K. Simons and W. L. C. Vaz, Annu. Rev. Biophys. Biomol. Struct. **33**, 269 (2004).

[10] M. J. W. Dodgson and M. A. Moore, Phys. Rev. B **55**, 3816 (1997).

[11] J. Thomson, Philos. Mag. **7**, 237 (1904).

[12] L. T. Wille, Nature (London) **324**, 46 (1986).

[13] T. Erber and G. M. Hockney, J. Phys. A **24**, L1369 (1991).

[14] E. L. Altschuler, T. J. Williams, E. R. Ratner, F. Dowla, and F. Wooten, Phys. Rev. Lett. **72**, 2671 (1994).

[15] T. Erber and G. M. Hockney, Phys. Rev. Lett. **74**, 1482 (1995).

[16] E. L. Altschuler, T. J. Williams, E. R. Ratner, R. Tipton, R. Stong, F. Dowla, and F. Wooten, Phys. Rev. Lett. **78**, 2681 (1997).

[17] J. R. Morris, D. M. Deaven, and K. M. Ho, Phys. Rev. B **53**, R1740 (1996).

[18] E. L. Altschuler and A. Pérez-Garrido, Phys. Rev. E **71**, 047703 (2005).

[19] E. L. Altschuler and A. Perez-Garrido, Phys. Rev. E **73**, 036108 (2006).

[20] F. H. Stillinger and T. A. Weber, Science **225**, 983 (1984).

[21] D. J. Wales and J. P. K. Doye, J. Chem. Phys. **119**, 12409 (2003).

[22] Z. Li and H. A. Scheraga, Proc. Natl. Acad. Sci. U.S.A. **84**, 6611 (1987).

[23] D. J. Wales and J. P. K. Doye, J. Phys. Chem. A **101**, 5111 (1997).

[24] D. J. Wales and H. A. Scheraga, Science **285**, 1368 (1999).

[25] D. J. Wales, *Energy Landscapes* (Cambridge University Press, Cambridge, England, 2003).

[26] M. Bowick, C. Cecka, and A. Middleton, http://tristis.phy.syr.edu/thomson/thomson.php

[27] Z. Li and H. A. Scheraga, J. Mol. Struct. **179**, 333 (1988).

[28] Http://www-wales.ch.cam.ac.uk/software.html

[29] D. J. Wales, J. P. K. Doye, *et al.*, The Cambridge Cluster Database, http://www-wales.ch.cam.ac.uk/CCD.html

[30] A. M. Livshits and Y. E. Lozovik, Chem. Phys. Lett. **314**, 577 (1999).

[31] M. J. Bowick, A. Cacciuto, D. R. Nelson, and A. Travesset, Phys. Rev. B **73**, 024115 (2006).

[32] M. J. Bowick, D. R. Nelson, and A. Travesset, Phys. Rev. B **62**, 8738 (2000).

[33] M. Bowick, A. Cacciuto, D. R. Nelson, and A. Travesset, Phys. Rev. Lett. **89**, 185502 (2002).

[34] L. J. Munro and D. J. Wales, Phys. Rev. B **59**, 3969 (1999).

[35] Y. Kumeda, L. J. Munro, and D. J. Wales, Chem. Phys. Lett. **341**, 185 (2001).

[36] U. Albrecht and P. Leiderer, J. Low Temp. Phys. **86**, 131 (1992).

[37] D. Pum, P. Messner, and U. B. Sleytr, J. Bacteriol. **173**, 6865 (1991).

[38] P. Lipowsky, M. J. Bowick, J. H. Meinke, D. R. Nelson, and A. R. Bausch, Nat. Mater. **4**, 407 (2005).

[39] M. J. W. Dodgson, J. Phys. A **29**, 2499 (1996).

[40] A. J. Stone and D. J. Wales, Chem. Phys. Lett. **128**, 501 (1986).

[41] H. F. Bettinger, B. I. Yakobsen, and G. E. Scuseria, J. Am. Chem. Soc. **125**, 5572 (2003).

[42] Y. Kumeda and D. J. Wales, Chem. Phys. Lett. **374**, 125 (2003).

[43] D. J. Wales, M. A. Miller, and T. R. Walsh, Nature (London) **394**, 758 (1998).

[44] T. R. Walsh and D. J. Wales, J. Chem. Phys. **109**, 6691 (1998).

[45] H. W. Kroto, J. R. Heath, S. C. O'Brien, R. F. Curl, and R. E. Smalley, Nature (London) **318**, 162 (1985).

[46] W. Krätschmer, L. D. Lamb, K. Fostiropoulos, and D. R. Huffman, Nature (London) **347**, 354 (1990).